



The Active Compensation Technique for Large Reflector Antennas Based on Quadratic Curve Fitting

Tian-Xiang Zheng¹, Bin-Bin Xiang¹ , Han-Wei Cui¹, Wei Wang² , Pei-Yuan Lian² , Shang-Ming Lin³ , Yang Zhang¹,
Jian-Ping Zhou¹, and Kai Li¹

¹ School of Mechanical Engineering, Xinjiang University, Urumqi 830017, China; xiangbinbin031@163.com

² School of Mechano-Electronic Engineering, Xidian University, Xi'an 710017, China

³ Xi'an Institute of Optics and Precision Mechanics, Chinese Academy of Sciences, Xi'an 710119, China

Received 2024 April 28; revised 2024 May 28; accepted 2024 June 4; published 2024 July 8

Abstract

Active reflectors are often used to compensate the surface distortion caused by environmental factors that degrade the electromagnetic performance of large high-frequency reflector antennas. This is crucial for maintaining high gain operation in antennas. A distortion compensation method for the active reflector of a large dual-reflector antenna is proposed. A relationship is established between the surface deformation and the optical path difference for the primary reflector by geometric optics. Subsequently, employing finite element analysis, a polynomial fitting approach is used to describe the impact of adjusting points on the reflector surface based on the coordinates of each node. By standardizing the positions of various panels on the reflector, the fitting ns can be applied to the reflector panels of similar shapes. Then, based on the distribution characteristics of the primary reflector panels, the adjustment equation for the actuators is derived by the influence matrix method. It can be used to determine the adjustment amount of actuators to reduce the rms of the optical path difference. And, the least squares method is employed to resolve the matrix equation. The example of a 110 m aperture dual-reflector antenna is carried out by finite element analysis and the proposed method. The results show that the optical path difference is reduced significantly at various elevation cases, which indicates that the proposed method is effective.

Key words: Methods: analytical – Methods: numerical – Telescopes

1. Introduction

A radio telescope is a device that uses a reflector antenna for the reception and transmission of radio waves in the context of astronomical research. The reflector antenna has the advantages of high efficiency, cost-effectiveness, lightweight components and broad frequency coverage (Samii & Haupt 2015). The Green Bank Telescope (GBT) is shown in Figure 1. Related technology finds extensive applications in various domains including radar systems, satellite communication, radio astronomy, remote sensing, bioelectronic technology and other fields. Nevertheless, due to the increase of the aperture area and its operating environment, the structure of the antenna is affected by the environment such as gravity, temperature and wind. These factors induce surface deformation on the reflector, consequently affecting the the electromagnetic (EM) performance of antennas (Baars 2020).

Numerous scholars have studied antenna reflector compensation technology in many papers. These approaches are typically classified into subreflector compensation and primary reflector compensation (Karcher 2006). The subreflector compensation adjusts five degrees of freedom to optimize the reflection path, while the primary reflector adjusts the position of the panel through multiple actuators. Hoerner (1981) studied the surface

deformation of a trapezoidal plate under strong torsion, providing a new idea for the research content of this paper. Wang and Xiang (Wang et al. 2014; Xiang et al. 2019b) proposed adjusting the subreflector to the focal point of the primary reflector to enhance the EM efficiency. The adjustment of the subreflector can compensate the deformation of the primary reflector on a significant level, and the adjustment accuracy of the active panel with multiple actuators is higher. Chen and Sun (Chen et al. 2015; Sun et al. 2021) conducted research on the impact of displacing the subreflector on antenna performance, and examined the pointing error resulting from the subreflector's offset. Stochino et al. (2017) optimized the finite element model of the Sardinia Radio Telescope (SRT) through photographic surveying, providing more accurate error data for surface compensation. Wang et al. (2017) proposed a method to calculate the amount of adjustment for the actuators from the perspective of electromechanical coupling. However, this method only considered the best-fitting reflector of the antenna, neglecting the elastic deformation of the panels. Hoferer & Samii (2002) proposed that the subreflector be parameterized by the coefficients of a global and orthogonal Fourier Jacobi set, which significantly reduces the number of parameters that need to be optimized. Bolli et al. (2014)



Figure 1. The GBT with an effective diameter of 100 m.

improved the performance of the antenna at the focal point of the subreflector by optimizing the profile of the dual-reflector of SRT. Zarghamee et al. (1995) introduced a computational algorithm for holographic technology that detects the variations in radio frequency path lengths and reduces the errors of adjustments resulting from actuators. Lian et al. (2019, 2021) installed a precise measuring instrument at the back of the subreflector to measure the distance and angle of elevation to a specified point on the primary reflector, which ensure the optimal position of the reflectors in real-time. Nevertheless, this method can only describe the margin of error at specific points. Alvarez et al. (2014) described the calibration process for the reflector being studied and performed a comparative evaluation of data processing methods using laser tracker and photographic surveying techniques. In brief, numerous scholars have proposed the compensation techniques for a reflector at various aspects. However, current methods for calculating the thousands of actuators lack a detailed discussion on EM properties. Additionally, most methods rely on the fitting surfaces for error correction, without considering the deformation of the panels themselves.

In this paper, a compensation method for the active reflector of a large dual-reflector antenna is proposed. First, the impact of the surface deformation on the EM performance is expressed by the optical path difference (OPD), which can directly represent the phase error of the antenna. Second, the finite element analysis (FEA) of a single panel is carried out, and the relationship between the position and influence coefficient of the nodes relative to the adjustment points is determined by polynomial regression analysis. Then, according to the fitting function and distribution characteristics of the primary reflector, the relationship between each panel and the adjustment point is

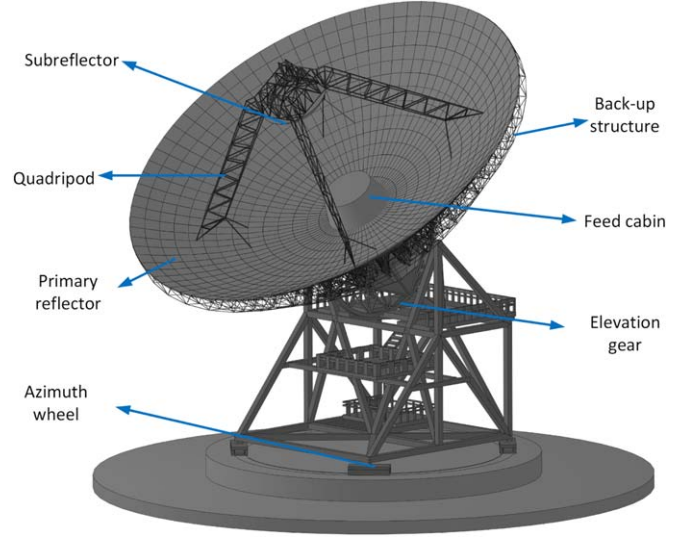


Figure 2. The structure of a radio telescope.

established. Finally, the mathematical model of minimizing OPD is established and calculated by the least squares method. The example of a 110 m aperture dual-reflector antenna is carried out by FEA and the proposed method to verify.

2. Optical Path Difference

The antenna is constantly affected by external factors during operation, which leads to bending and distortion of the reflector and reduces EM performance. In order to compensate the loss performance of the radio telescope quickly, it is necessary to analyze the error characteristics of the reflector, so as to establish an effective compensation method.

Figure 2 illustrates the basic components of a dual-reflector antenna. The deformation of back-up structure will cause the phase error of the aperture surface, which will reduce the EM performance of the antenna. As diagrammed in Figure 3, a plane wave can be reflected to the focal point of the primary reflector under the ideal state, and then be reflected to the feed cabin by the subreflector. F is the focal point of the primary reflector, f is the focal length, C is a random point on the ideal reflector, r is the radius, and θ is the half-angle of the point. According to the theory of geometric optics, the radio wave that originally passed through point C will be moved to A due to the deformation of the panel. The difference in distance between radio waves throughout the reflection process is called the OPD, which is

$$\varepsilon_m = \varepsilon_1 + \varepsilon_3 = \varepsilon_1 + \varepsilon_1 \cos \theta = \varepsilon_1(1 + \cos \theta). \quad (1)$$

The OPD can reflect the phase error of the near field, which can be expressed as

$$\delta_m = \frac{2\pi}{\lambda} \varepsilon_1(1 + \cos \theta), \quad (2)$$

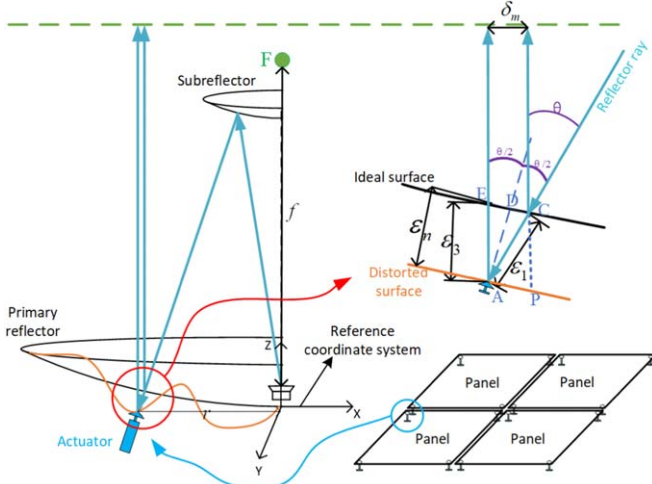


Figure 3. The primary reflector distortion causes the OPD.

where λ is the wavelength, and δ_m is the phase error caused by the deformation of the primary reflector. The phase error will lead a change of the radiation pattern, resulting in a decrease of the main lobe and an increase of the side lobe. Therefore, the EM performance of the antenna can be improved indirectly by reducing the OPD at the reflector.

In practical applications, the root mean square (rms) of the half-OPD is used to assess the focusing performance of the primary reflector. According to the geometric relationship in Figure 3, the relationship between the half-OPD and the normal or axial error can be obtained as follows

$$\frac{\varepsilon_m}{2} = \varepsilon_1 \cos^2 \frac{\theta}{2} = \varepsilon_3 \cos^2 \frac{\theta}{2} = \varepsilon_n \cos \frac{\theta}{2}, \quad (3)$$

which can be expressed in terms of radius and focal length as

$$\frac{\varepsilon_m}{2} = \varepsilon_1 \frac{4f^2}{4f^2 + y^2} = \frac{\varepsilon_n}{\sqrt{1 + \left(\frac{r}{2f}\right)^2}}. \quad (4)$$

The phase error of a double reflector antenna is the result of the primary reflector, the subreflector and the feed error. The focus of this paper is the active compensation method for the primary reflector. Hence, it can be assumed that the subreflector is located in the optimal position. Therefore, there is no effect on the final receiving efficiency of the antenna, and it is considered as feed. According to the aforementioned theory, the OPD resulting from the deformation of the primary reflector can be calculated, and the influence of the surface distortion on received intensity can be reduced by minimizing the OPD.

3. Active Adjustment of the Primary Reflector

The operation of the reflector antenna has high precision requirements for the motion of elevation and azimuth. To

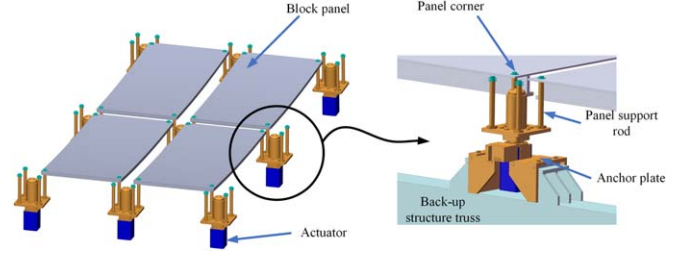


Figure 4. The active panel of the primary reflector with actuators.

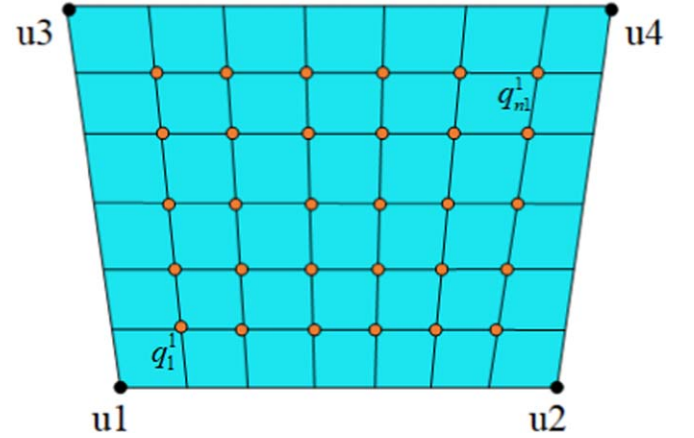


Figure 5. Finite element model for one panel.

guarantee the stability of operations, the majority of radio telescopes are calibrated using mechanical transmission, and the primary reflector uses shared actuators to increase cost-effectiveness and operational efficiency. An adjustment mechanism is linked to either two or four neighboring panels, with each panel being strengthened by a stiffener located at the bottom. The adjustments of the panels are implemented by driving the extension of the four actuators, and the actuators are fixed to the back-up structure as shown in the Figure 4. Typically, the adjustment direction of the actuators is the normal direction of the adjustment point.

3.1. Reflector Panel Analysis

In order to establish the relationship between the adjustment amount of actuators and the surface deformation of the primary reflector, a single active panel is analyzed first. As illustrated in the Figure 5, a finite element model of a primary reflector panel has four adjustment points, where u_1 , u_2 , u_3 and u_4 are the adjustment amounts of the four actuators of the panel. The distribution of nodes in the panel can be obtained through grid division, where $q_1(x_1, y_1)$ and $q_{n1}(x_{n1}, y_{n1})$ represent the coordinate values of the first node and the $n1$ node respectively, and $n1$ is the maximum number of nodes in the panel. The

density of the meshing will determine the precision of panel analysis and adjustment.

The deformation of the panel can be improved by adjusting the four actuators. According to the principle of linear superposition, it can be inferred that the distortion of the panel is the combined effects of the four adjustment points. Therefore, each node in the panel can be considered to have a unique influence coefficient relative to the four adjustment points, which can be expressed as

$$\delta_i = u_1 \times \lambda_i^1 + u_2 \times \lambda_i^2 + u_3 \times \lambda_i^3 + u_4 \times \lambda_i^4, \quad (5)$$

where δ_i is the deformation of the i -th node in the panel, and λ_i^1 is the influence coefficient of the first adjustment point on the i -th node. According to Equation (5), the deformation of a panel resulting from the adjustment point can be accurately depicted by determining the influence coefficient of each node in relation to the adjustment point.

The influence coefficient directly reflects the degree of correlation between nodes and adjustment points, while the number of nodes reflects the accuracy of surface shape. In general, a higher mesh density in the panel will improve the solution accuracy. In order to obtain the optimal adjustment quickly, the influence coefficients associated with the nodes' coordinates are established through polynomial regression.

Polynomial regression is a versatile method that can effectively model irregular and nonlinear data sets, providing a more accurate fit for data exhibiting diverse shapes. By changing the order of the polynomial, the complexity and adaptability of the fitting process can be adjusted.

The deformation of the panel caused by a single adjustment point can be expressed by the amount of adjustment points and the coordinates of nodes. Due to the special structure of the panel, the deformation of a panel caused by the adjustment point cannot be described by a single geometric formula. We can represent the influence coefficient of the adjustment point 1 corresponding to each node as follows

$$[\lambda_1, \lambda_2, \dots, \lambda_{n_1}]^T = \left[\frac{\delta_1}{u_1}, \frac{\delta_2}{u_1}, \dots, \frac{\delta_{n_1}}{u_1} \right]^T, \quad (6)$$

where u_1 is the amount of adjustment for a adjustment point. Due to the amount of adjustment actuators being very small relative to the size of the panel, in the same panel, the influence coefficients of the nodes are almost equal for different adjustments. Therefore, it is possible to represent the influence coefficients using the coordinates of nodes in the plane

$$[\lambda_1, \dots, \lambda_{n_1}]^T = [f(x_1, y_1), \dots, f(x_{n_1}, y_{n_1})]^T, \quad (7)$$

where x_1, y_1 is the coordinates of the first node, and $f(x_1, y_1)$ is the fitting function of the first node corresponding to the first adjustment point. FEA shows that the panel deformation caused by an adjustment point is a convex surface. Therefore, the surface shape can be fitted by using a quadratic polynomial. In order to solve the optimal fitting coefficient, the

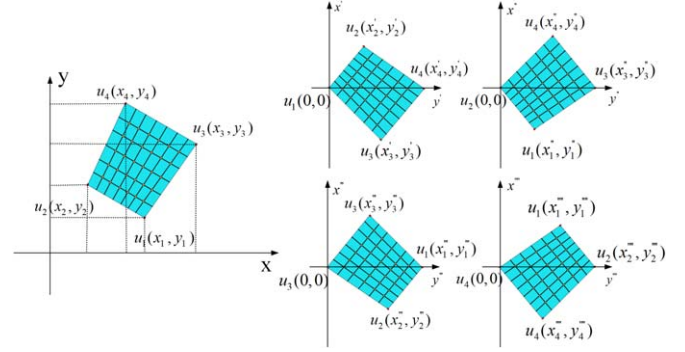


Figure 6. Rotate the panel based on the adjustment point.

corresponding mathematical model can be established and expressed as

$$\begin{aligned} f(x, y) &= ax^2 + by^2 + cxy + dx + ey + f \\ \text{find} : & a, b, c, d, e, f \\ \text{min} : & \text{rms} \left(\sum_{i=1}^{n_1} f(x_i, y_i) - \lambda_i \right) \\ \text{s.t.} : & 0 \leq x_i \leq x_{\max}, 0 \leq y_i \leq y_{\max}, \end{aligned} \quad (8)$$

where a, b, c, d, e and f are the coefficients of $f(x, y)$, and λ_i represents the influence coefficient of each node obtained by FEA.

Due to the node coordinates of the panel being different in the primary reflector, it is impossible to establish a corresponding functional relationship in the global coordinate system. Here, we standardize the position according to the structural characteristics of the panel. As demonstrated in Figure 6, the conversion of coordinates for a single panel involves four adjustment points. This process includes establishing a local coordinate system for each adjustment point and designating the adjustment point with the greatest distance as the y -axis. Consequently, the local coordinates of the nodes in the respective local coordinate system are obtained. By quadratic fitting the influence coefficients in the local coordinate system, the influence relationship can be represented by four fitting functions:

$$\begin{aligned} [\lambda_1^1, \dots, \lambda_{n_1}^1]^T &= [f_1(x_1^1, y_1^1), \dots, f_1(x_{n_1}^1, y_{n_1}^1)] \\ [\lambda_1^2, \dots, \lambda_{n_1}^2]^T &= [f_2(x_1^2, y_1^2), \dots, f_2(x_{n_1}^2, y_{n_1}^2)] \\ [\lambda_1^3, \dots, \lambda_{n_1}^3]^T &= [f_3(x_1^3, y_1^3), \dots, f_3(x_{n_1}^3, y_{n_1}^3)] \\ [\lambda_1^4, \dots, \lambda_{n_1}^4]^T &= [f_4(x_1^4, y_1^4), \dots, f_4(x_{n_1}^4, y_{n_1}^4)]. \end{aligned} \quad (9)$$

This method can reduce the fitting error caused by the change of coordinates of the panel and improve the accuracy of the fitting results. Based on the four influence functions, we can

represent all nodes of a panel in the form of a matrix

$$s = \begin{bmatrix} \delta_1 \\ \delta_2 \\ \vdots \\ \delta_{n_1} \end{bmatrix} = \begin{bmatrix} f_1^1 & f_1^2 & f_1^3 & f_1^4 \\ f_2^1 & f_2^2 & f_2^3 & f_2^4 \\ \vdots & \vdots & \vdots & \vdots \\ f_{n_1}^1 & f_{n_1}^2 & f_{n_1}^3 & f_{n_1}^4 \end{bmatrix} \begin{bmatrix} u_1 \\ u_2 \\ u_3 \\ u_4 \end{bmatrix} = F_{n_1} u, \quad (10)$$

where F_{n_1} is the influence matrix of the panel, u is the normal adjustment vector, and s is the normal deformation vector of the nodes in the panel caused by the adjustment of the actuators.

As drawn in Figure 3, considering that the panel is a component located in the primary reflector, the distortion of the panel will lead to OPD. According to Equation (4), in order to obtain the OPD of the node, it is necessary to obtain the radius of the node located in the primary reflector, which can be expressed as follows

$$g = \delta \times \frac{2}{\sqrt{1 + \left(\frac{r}{2f}\right)^2}} = \delta \times t, \quad (11)$$

where g is the OPD of the node, and t is the conversion coefficient of the OPD. This extends to the entire panel, denoted as

$$g = \begin{bmatrix} g_1 \\ g_2 \\ \vdots \\ g_{n_1} \end{bmatrix} = \begin{bmatrix} t_1 & 0 & \dots & 0 \\ 0 & t_2 & \dots & 0 \\ \vdots & \vdots & \ddots & \vdots \\ 0 & 0 & \dots & t_{n_1} \end{bmatrix} \times F_{n_1} \times u = T_{n_1} F_{n_1} u, \quad (12)$$

where t_{n_1} is the OPD conversion coefficient of the n_1 node, T is the OPD conversion matrix, which is a diagonal matrix, g is the OPD vector of the nodes, and F is the influence matrix. Each influence coefficient can be obtained from the two-dimensional coordinates of the panel nodes in the local coordinate system. Through the above equation, we can get the relationship between the adjustment of four adjustment points and the OPD of the panel.

3.2. Influence Matrix of the Primary Reflector

In general, the panels of the primary reflector are distributed along the circumference of the ring, and the panels of each ring are the same size. In order to ensure the stability of panel adjustment, the number of panels on the ring will increase correspondingly with the increase of the rings. As shown in Figure 7, each panel is adjusted by four shared actuators. An actuator adjusts four adjacent panels, with the innermost or outermost circle of the panels consisting of two panels.

To calculate the total amount of adjustment for shared actuators simultaneously, it is essential to describe the relationship between the nodes and the adjustment points of all panels according to the distribution of the panels. As shown in Figure 7, we assume the influence coefficient of the first

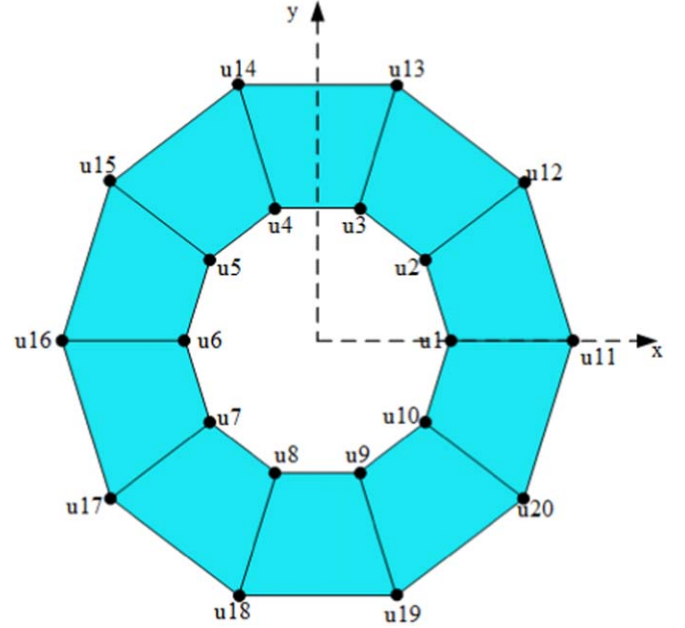


Figure 7. A ring of 10 panels in the primary reflector.

adjustment point relative to all nodes in the first panel is represented as $f^{(1,1)} = [f_1^{(1,1)}, f_2^{(1,1)}, \dots, f_{n_1}^{(1,1)}]^T$, where n_1 is the number of nodes in the first panel. The influence matrix of the ring can be expressed as

$$F_1 = \begin{bmatrix} f^{(1,1)} & f^{(2,1)} & & f^{(11,1)} & f^{(12,1)} & & \\ & \ddots & \ddots & & \ddots & \ddots & \\ & & f^{(10,10)} & f^{(11,10)} & & & \\ f^{(1,10)} & & & & & & f^{(20,10)} \end{bmatrix}, \quad (13)$$

where the number of rows is the number of nodes n^1 in the panel, $n^1 = n_1 + n_2 + \dots + n_{10}$, and the number of columns is the number of adjustment points. Therefore, we assume that the first ring has i adjustment points and j panels, then its influence matrix can be written

$$F_1 = \begin{bmatrix} f^{(1,1)} & f^{(2,1)} & & f^{(\frac{i}{2}+1,1)} & f^{(\frac{i}{2}+2,1)} & & \\ & \ddots & \ddots & & \ddots & \ddots & \\ & & f^{(\frac{i}{2},j)} & f^{(\frac{i}{2}+1,j)} & & & f^{(i,j)} \end{bmatrix}. \quad (14)$$

The optical path conversion matrix is

$$T_1 = \begin{bmatrix} t_1 & & & & \\ & t_2 & & & \\ & & \ddots & & \\ & & & \ddots & \\ & & & & t_{n^1} \end{bmatrix}, \quad (15)$$

where t_{n^1} is the OPD conversion coefficient of the n_1 node. Based on the above matrix, the relationship between the

amount of adjustment for each adjustment point and the OPD of the nodes can be deduced as follows

$$g_1 = T_1 \times F_1 \times u_i, \quad (16)$$

where $u_i = [u_1, u_2, \dots, u_{\text{end}}]^T$ is the amount of adjustment for the ring, and g_1 is the OPD vector. It can be inferred that the relationship between all adjustment points and OPD of the entire primary reflector is

$$g_{\text{all}} = \begin{bmatrix} g_1 \\ g_2 \\ \vdots \\ g_m \end{bmatrix} = \begin{bmatrix} T_1 & & & \\ & T_2 & & \\ & & \ddots & \\ & & & T_m \end{bmatrix} \times \begin{bmatrix} F_1 & & & \\ & F_2 & & \\ & & \ddots & \\ & & & F_m \end{bmatrix} \times \begin{bmatrix} u_1 \\ u_2 \\ \vdots \\ u_{\text{end}} \end{bmatrix} = TFu, \quad (17)$$

where T is the OPD conversion matrix of all nodes, F is the influence matrix of the primary reflector, and m is the number of rings in the reflector.

4. Optimal Amount of Adjustment

The thousands of actuators on the primary reflector are adjusted simultaneously. We assume that δ_a is the normal deformation vector of nodes in the finite element model of the primary reflector, g_a is the OPD caused by deformation, and g_u is the OPD caused by the adjustment of actuators. Therefore, the OPD after adjusting can be expressed as

$$\Delta = g_a + g_u = T\delta_a + TFu, \quad (18)$$

where T , F , and u are the same as expressed in Equation (17). In order to calculate the amount of adjustment for all actuators at once, we can establish mathematical models, which can be expressed as

$$\begin{aligned} &\text{find: } u \\ &\text{min: } \text{rms}(\Delta) \\ &\text{s.t.: } u_{\min} \leq u_i \leq u_{\max}, \end{aligned} \quad (19)$$

where u_{\min} and u_{\max} are the minimum and maximum boundaries of adjustment u_i respectively. Since Δ is a set of node vectors, the rms can be represented by vector multiplication

$$\text{rms}(\Delta) = \sqrt{\frac{\Delta^T \Delta}{N}}, \quad (20)$$

where N is the number of nodes of the primary reflector.

The iterative approach is commonly used to resolve the aforementioned mathematical model. Nevertheless, a large number of adjustment points can take up computation time and computer memory. Therefore, the least squares method is

utilized for the purpose of approximate calculations

$$e = N \times \|\text{rms}(\Delta)\| = \delta_a^T T^T TFu + \delta_a^T T^T T\delta_a + u^T F^T T^T TFu + u^T F^T T^T TS. \quad (21)$$

The optimal adjustment u should meet

$$\frac{\partial e(u)}{\partial u} = 2F^T T^T (TFu + T\delta) = 0. \quad (22)$$

The solution of Equation (22) is the optimal adjustment displacement of the actuators, which can be expressed as

$$u = -(F^T T^T TF)^{-1} F^T T^T T\delta_a. \quad (23)$$

The optimal adjustment response equation is established by the least squares method. The OPD of the primary reflector after adjustment can be obtained by combining the optimal adjustment with Equation (18). Since the polynomial function is used to determine the optimal deformation surface, the elastic deformation and the variation of the panel size are considered. The obtained findings exhibit a high level of concordance with the outcomes derived from FEA.

5. Numerical Results and Discussion

To assess the efficacy of the proposed method, a finite element model of the 110 m primary reflector was used to verify the method through simulation. It should be noted that the data described in this paper are obtained by finite element simulation. Since the main focus of this paper is on calculating the optimal adjustment amount based on known errors, we only consider the deformation of the primary reflector under gravity load. As shown in the Figure 8, the primary reflector of the dual-reflector antenna has 20 rings. The panels of each ring are equipped with shared actuators for adjustment, and the panels of adjacent rings share one actuator ring. The adjustment points are located at four corner points of the panels, and the reflector deformation is compensated by adjusting the extension of the actuator.

First, a single panel is analyzed to determine the deformation caused by the displacement of its four corner points. Then, the local coordinates of each panel are defined to derive the influence fitting function. Subsequently, the deformations of the primary reflector at 90° and 10° are analyzed by the finite element model. Based on the influence matrix derived in this paper, the optimum adjustments of the actuators are calculated and the OPD is corrected. The effectiveness of the method used in this paper was verified by comparing with the traditional method.

5.1. Panel Fitting Analysis

Taking the panel of the 14th ring of the primary reflector as an example, the influence coefficients of the panel nodes are fitted by quadratic polynomial. The adjustment points of the panel are illustrated in Figure 5. We apply the displacement constraints of corner points to the adjustment points u_1 , u_2 , u_3 and u_4 in turn. Then, we can obtain the distribution of the

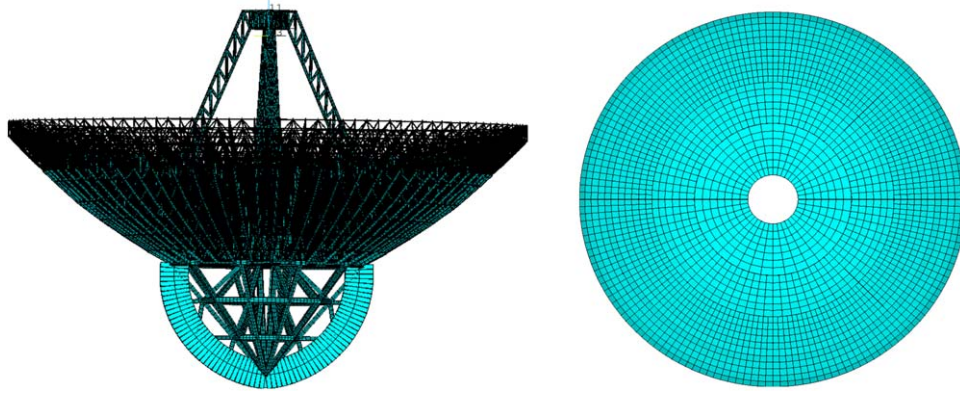


Figure 8. The finite element model and panel distribution of the 110 m primary reflector.

influence coefficient of nodes for different adjustment points and rotate it to the local coordinate system as depicted in Figure 9. It can be seen that the distributions of influence coefficients in the four cases are different; the closer to the position of the adjustment point, the greater influence coefficient of the node. The specific size of the influence coefficient is related to the angle and length of the adjacent edge and the material of the panel.

By obtaining the influence coefficients at different cases of a single panel, we can use the quadratic polynomial to fit the influence coefficients of the four cases, and the fitting function is the same as Equation (8). The fitting coefficients of the four fitting functions are shown in Table 1. The independent variables of each equation are the local coordinates of the current panel, and the last column is the fitting error of the panel with a constraint of 10 mm. Due to the different shapes of the 110 m reflector panels, the panels of rings 1, 9, 12, 14, 15 and 19 were fitted separately in this paper to reduce the influence of fitting errors. The fitting error of nodes on the panel are plotted in Figure 10.

The quadratic polynomial fitting method can accurately obtain the deformation caused by a single adjustment point in the local coordinate system; the more similar the panels, the smaller the fitting error. Therefore, six influence functions are fitted to the primary reflector in order to minimize the influence of fitting error in this paper.

5.2. Optimal Amount of Adjustment

Through FEA of 110 m the primary reflector model, the shape accuracy of the reflector surface is improved by adjusting the actuator, thereby enhancing the EM performance of the antenna. In this paper, the state of 90° and 10° elevations of the primary reflector is compensated. By calculating the amount of adjustment for the actuators, the traditional method and what is proposed in this paper are compared. The traditional method takes the normal deformation at the adjustment points as the

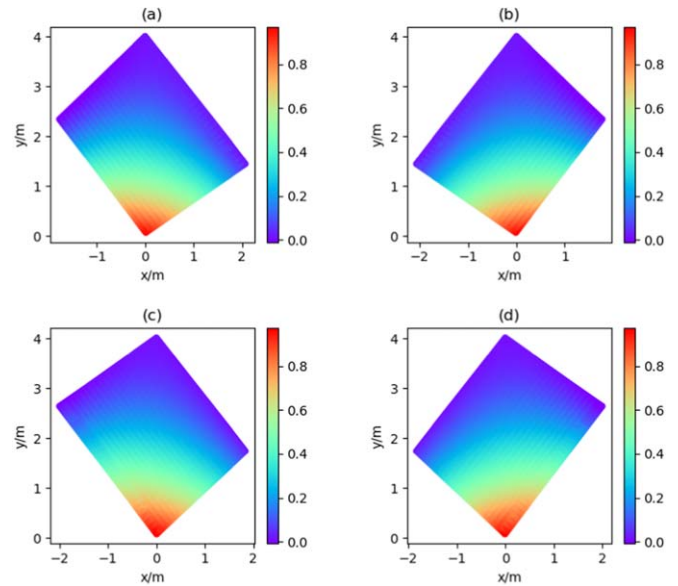


Figure 9. The distribution of influence coefficients of each node in the panel.

amount of adjustment. The method proposed in this paper is based on a quadratic polynomial to get the amount of adjustment for actuators. The surface error after adjustment can be calculated by the Equation (18).

The primary reflector of the 110 m antenna has 1920 panels and 2048 shared actuators, and a large number of nodes are generated after meshing. According to Equation (17), the influence matrix can be expressed as a sparse banded matrix, and the calculation by a sparse matrix can speed up the computation. As plotted in Figure 11, a sparse matrix diagram representing the influence coefficient for the primary reflector is presented. Region *a* is the influence matrix from rings 1 to 4, region *b* is the influence matrix from rings 5 to 8, and region *c* is the influence matrix from rings 9 to 20.

Table 2 lists the rms of the primary reflector at 90° and 10° using different methods. The rms of the primary reflector before

Table 1
The Fitting Parameters of Adjustment Points

Cases	a	b	c	d	e	f	rms/ μm
u1	-0.063	0.062	-0.037	0.15	-0.509	1.063	64.5
u2	-0.063	0.062	0.037	-0.15	-0.509	1.032	64.5
u3	-0.058	0.059	0.035	-0.13	-0.502	1.016	55.06
u4	-0.058	0.059	-0.035	0.131	-0.502	1.039	55.06

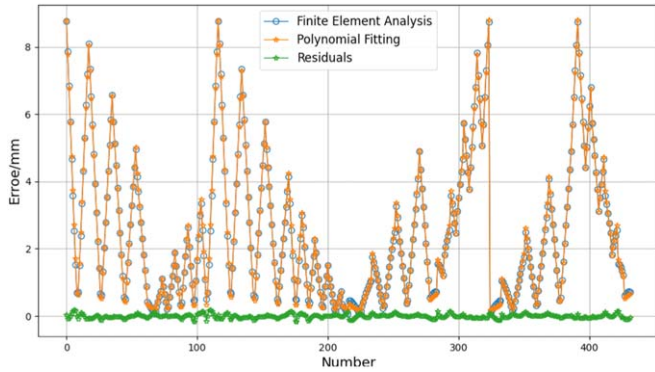


Figure 10. Deformation of nodes in the 14th ring panel.

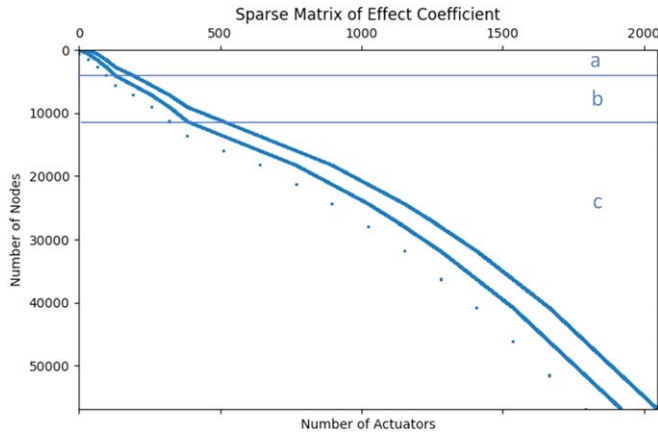


Figure 11. Sparse matrix of influence coefficient of 110 m primary reflector.

adjustment is obtained by FEA. Figure 12 visualizes the surface error distribution corresponding to different directions on the primary reflector. Figures 13 and 14 show the OPD using the present method and the traditional method at 10° and 90° elevation angles after adjustment, respectively. When the elevation angle of the primary reflector is 90° , the rms is 4.947 mm before adjustment, and the rms of the traditional and the proposed method is reduced to 0.7129 mm and 0.0578 mm after adjustment, respectively. Although both methods yield reasonable performance, the method used in this paper shows better performance than the traditional method. When the elevation

Table 2
rms Errors of the Reflector Surface before and after Adjustment

Terms	B-A	T-M	P-M
10°	9.21 mm	1.3113 mm	0.1022 mm
90°	4.947 mm	0.7129 mm	0.0578 mm

Note. B-A, T-M and P-M denote before adjustment, traditional method and proposed method, respectively.

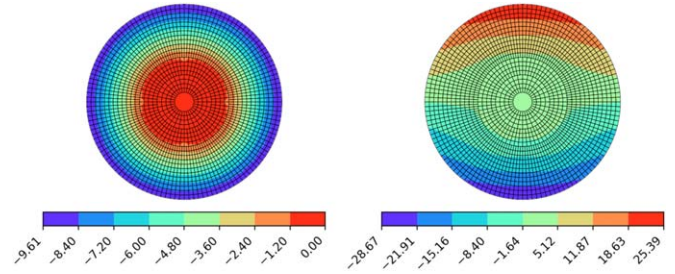


Figure 12. Deformation of the primary reflector at 90° (left) and 10° (right).

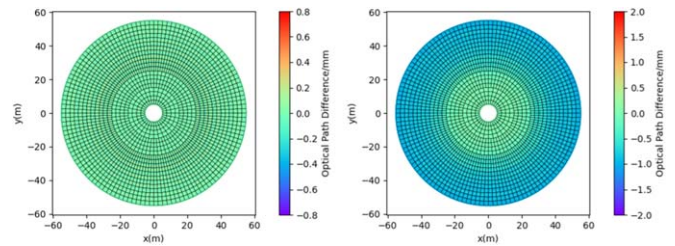


Figure 13. OPD distribution when the reflector elevation is 90° . After adjustment using the method in this paper (left) and the traditional one (right).

angle of the primary reflector is 10° , the optimization results are similar.

Through the surface error analysis and compensation of the primary reflector, the EM performance of the primary reflector is analyzed at 24 GHz (Xiang et al. 2019a). As demonstrated in Figures 15 and 16, the amplitude direction diagram of the primary reflector shows the effect of different compensation methods on the electrical properties. Each elevation angle determines the section pattern in both horizontal and vertical directions. When the elevation angle of the primary reflector is 90° , the main lobe drops seriously in the horizontal direction

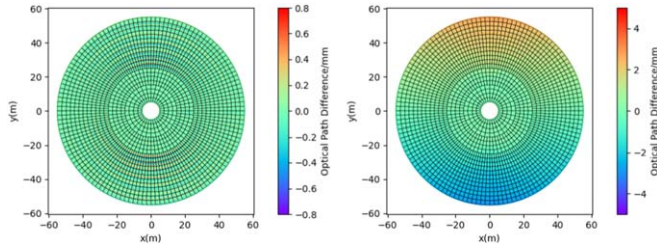


Figure 14. OPD distribution when the reflector elevation is 10° . After adjustment using the method in this paper (left) and the traditional one (right).

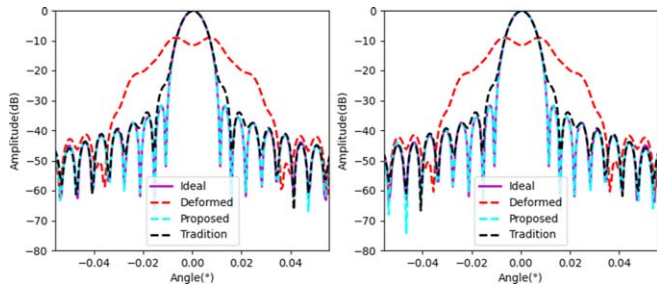


Figure 15. The horizontal (left) and vertical (right) far-field at 90° .

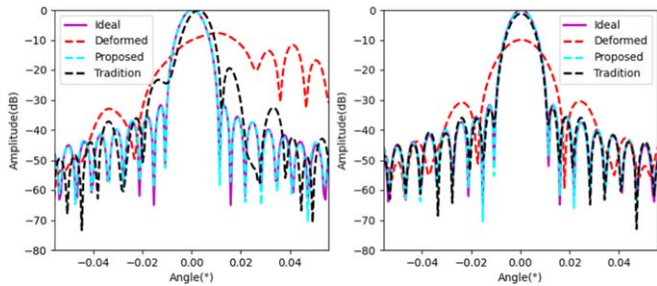


Figure 16. The horizontal (left) and vertical (right) far-field at 10° .

and the vertical direction, and the amplitude is -9.028 dB. The amplitude is reduced to -0.142 dB by the traditional method after adjustment, and can be reduced to -0.0037 dB by the method proposed in this paper. When the elevation angle is 10° , the amplitude of horizontal direction and vertical direction is -7.711 dB and -9.948 dB, respectively. The amplitude adjusted by the traditional method is -0.127 dB and -1.185 dB, and the amplitude adjusted by the method used in this paper is -0.011 dB. In summary, the amplitude pattern adjusted by the method in this paper has a high consistency with the ideal pattern, which is significantly improved compared with the traditional method.

6. Discussion

In this paper, a new method for compensating the primary reflector of a large aperture antenna is presented. The method

considers the distortion of the reflector panel caused by actuators, and describes the influence coefficient of the adjustment point on the single panel in global coordinates based on the quadratic polynomial. The corresponding local coordinate system is established for all panels, and the adjacent panels are adapted to the fitting function by standardization. Based on the fitting function of six panels of different sizes, the relationship between the adjustment of actuators and the OPD of the primary reflector is established by the influence matrix method. Finally, the least squares method is used to determine the amount of adjustment for all actuators at once. According to the amplitude pattern of the primary reflector, this method has higher adjustment precision than the traditional method. The EM performance of the antenna can be significantly improved by minimizing the rms of the OPD, which indicates that the proposed method is effective.

Acknowledgments

This research was funded by the National Natural Science Foundation of China (NSFC, grant Nos. 12363011, 52275270, and 52275269), Natural Science Foundation of Xinjiang Uygur Autonomous Region (No. 2023D01C22), the Tianchi Talents Program of Xinjiang, the National Key Basic Research Program of China (No. 2021YFC2203501) and the Xinjiang Postdoctoral Foundation.

ORCID iDs

Bin-Bin Xiang  <https://orcid.org/0000-0001-7071-4779>
 Wei Wang  <https://orcid.org/0000-0003-1667-570X>
 Pei-Yuan Lian  <https://orcid.org/0000-0002-8461-0169>
 Shang-Ming Lin  <https://orcid.org/0000-0002-3995-2354>

References

- Alvarez, M. L., Torres, C. T., Rios, E. H., et al. 2014, *Proc. SPIE*, **9151**, 91513S
 Baars, J. W. 2020, *URSB*, **2020**, 10
 Bolli, P., Olmi, L., Roda, J., & Zaccchioli, G. 2014, *IAWPL*, **13**, 1713
 Chen, L., Sun, Z.-X., Wang, J.-Q., Wan, G.-H., & Tong, M.-S. 2015, *PIERM*, **44**, 59
 Hoerner, V. S. 1981, *ITAP*, **29**, 953
 Hoferer, R. A., & Samii, R. Y. 2002, *ITAP*, **50**, 1676
 Karcher, H. J. 2006, *IAPM*, **48**, 17
 Lian, P.-Y., Wang, C.-S., Xue, S., et al. 2021, *ITAP*, **69**, 6351
 Lian, P.-Y., Wang, C.-S., Xue, S., et al. 2019, *IET Microwaves Antennas & Propagation*, **13**, 2669
 Samii, R. Y., & Haupt, R. 2015, *IAPM*, **57**, 85
 Stochino, F., Cazzani, A., Poppi, S., & Turco, E. 2017, *MMS*, **22**, 885
 Sun, Z.-X., Wang, J.-Q., Yu, L.-F., Wei Gou, W., & Wang, G.-L. 2021, *RAA*, **21**, 038
 Wang, C.-S., Lan, X., Wang, W., et al. 2017, *RAA*, **17**, 043
 Wang, W., Wang, C.-S., Duan, B.-Y., Leng, G.-J., & Li, X.-P. 2014, *IET Microw. Antennas Propag.*, **8**, 158
 Xiang, B.-B., Wang, C.-S., & Lian, P.-Y. 2019a, *Int. J. Antennas Propagation*, **2019**, 15
 Xiang, B.-B., Wang, C.-S., Lian, P. Y., Wang, N., & Ban, Y. 2019b, *RAA*, **19**, 062
 Zarghamee, M. S., Antebi, J., & Kan, F. W. 1995, *ITAP*, **43**, 79